Physiological Reports

Open Access

ORIGINAL RESEARCH

Effects of acid-base variables and the role of carbonic anhydrase on oxalate secretion by the mouse intestine in vitro

Jonathan M. Whittamore[1], Susan C. Frost[2] & Marguerite Hatch[1]

1 Department of Pathology, Immunology and Laboratory Medicine, College of Medicine, University of Florida, Gainesville, Florida, USA
2 Department of Biochemistry and Molecular Biology, College of Medicine, University of Florida, Gainesville, Florida, USA

Keywords
Anion exchange, bicarbonate, chloride, CO_2, colon, ileum, pH.

Correspondence
Jonathan M. Whittamore, Department of Pathology, Immunology and Laboratory Medicine, College of Medicine, University of Florida, Gainesville, FL 32610, USA.
Tel: (352)-392-3045
Fax: (352)-273-3053
E-mail: j.m.whittamore@pathology.ufl.edu

Funding Information
This work was supported by National Institute of Diabetes and Digestive and Kidney Diseases (NIDDK) grants DK-088892 and U54 DK-083908 from the National Institutes of Health.

Received: 17 October 2014; Revised: 6 December 2014; Accepted: 30 December 2014

doi: 10.14814/phy2.12282

Physiol Rep, 3 (2), 2015, e12282, doi: 10.14814/phy2.12282

Abstract

Hyperoxaluria is a major risk factor for calcium oxalate kidney stones and the intestine is recognized as an important extra-renal pathway for eliminating oxalate. The membrane-bound chloride/bicarbonate (Cl^-/HCO_3^-) exchangers are involved in the transcellular movement of oxalate, but little is understood about how they might be regulated. HCO_3^-, CO_2, and pH are established modulators of intestinal NaCl cotransport, involving Na^+/H^+ and Cl^-/HCO_3^- exchange, but their influence on oxalate transport is unknown. Measuring ^{14}C-oxalate and ^{36}Cl fluxes across isolated, short-circuited segments of the mouse distal ileum and distal colon we examined the role of these acid-base variables and carbonic anhydrase (CA) in oxalate and Cl^- transport. In standard buffer both segments performed net oxalate secretion (and Cl

intestinal oxalate transport and overall homeostasis to be defined.

In the small intestine, PAT1 (Putative Anion Transporter 1; Slc26a6) is a Cl^-/HCO_3^- exchanger expressed predominantly in the small intestine, located in the apical membrane of the villus epithelium, with roles in nutrient and nonnutrient-linked Cl^- absorption, as well as HCO_3^- secretion and absorption, and intracellular pH regulation (Wang et al. 2002, 2005; Simpson et al. 2007, 2010; Singh et al. 2008, 2010; Walker et al. 2011; Xia et al. 2014). Studies of PAT1-KO mice have shown this transporter is also involved in oxalate secretion by the duodenum (Jiang et al. 2006) and ileum (Freel et al. 2006). Another important apical Cl^-/HCO_3^- exchanger is DRA (Down-Regulated in Adenoma; Slc26a3), which is prominently involved in Cl^- absorption and HCO_3^- secretion along the length of the intestine (Walker et al. 2008; Singh et al. 2010; Freel et al. 2013; Whittamore et al. 2013; Xia et al. 2014; Xiao et al. 2014). Most recently, using DRA-KO mice we have shown that DRA also contributes to oxalate absorption by the ileum, cecum, and distal colon (Freel et al. 2013). The development of transgenic mice for these transporters has revealed the tremendous value of such animal models for advancing our understanding of intestinal oxalate transport and the roles of individual anion exchangers. Yet, there remains scant information on some of the overall fundamental oxalate-transporting characteristics of the mouse intestine, and furthermore how they might be regulated. Such knowledge will aid a better understanding of the patho-physiology behind disorders of oxalate metabolism, and is vital given the interest in developing the therapeutic potential of the intestine as a means to combat hyperoxaluria (Hatch et al. 2011; Robijn et al. 2011).

One of the most essential functions of the apical Cl^-/HCO_3^- exchangers in the intestine occurs when coupled with sodium/proton (Na^+/H^+) exchange to perform electroneutral NaCl and fluid absorption. This is a highly regulated process and a broad range of hormonal, immune, and nervous system inputs can modify and coordinate NaCl cotransport and HCO_3^- secretion by the intestine in a segment-specific manner (Kato and Romero 2011). The effects on Na^+/H^+ and Cl^-/HCO_3^- exchange activity in the ileum and colon in response to alterations in systemic acid-base homeostasis has previously been established for humans, rats, and rabbits in vivo and in vitro (Charney and Feldman 1984; Charney et al. 1995; Charney and Dagher 1996; Gennari and Weise 2008), and subsequently for mice in vitro (Goldfarb et al. 2000; Charney et al. 2004b). Elegant studies on the acute effects of CO_2 in the rat distal colon demonstrated rapid shifts in the expression of these transporters at the apical membrane signaled through intracellular pH and $[HCO_3^-]$, mediated by the catalytic enzyme carbonic anhydrase (CA) (Charney et al. 2002b, 2004a). The components of the bicarbonate buffering system (pH, HCO_3^- and CO_2) therefore represent additional, and often overlooked, regulatory factors controlling intestinal electrolyte transport (Goldfarb et al. 1988; Charney and Dagher 1996), but their effects on oxalate handling have not been considered. As oxalate is a substrate of the Cl^-/HCO_3^- exchangers, we hypothesized that it too would display characteristics of being modified and regulated by these acid-base variables. The aim of this study was therefore to systematically examine how changes to pH, HCO_3^- and CO_2 impact oxalate transport by the mouse intestine in vitro. Given we know relatively more about intestinal Cl^- transport than oxalate, and because Cl^- is one of the primary substrates of the anion exchangers, collecting information on the associated Cl^- fluxes as part of these investigations offered a useful reference for interpreting the responses of oxalate in the context of what we presently understand about Cl^- transport. The following study reports how oxalate and Cl^- fluxes across the mouse distal ileum and distal colon were affected by alterations in acid-base variables and the role of CA.

Materials and Methods

Experimental animals

The following experiments used the wild-type (WT) C57BL/6 mouse strain. All mice were from breeding colonies housed at the AAALAC (Association for Assessment and Accreditation of Laboratory Animal Care)-accredited animal facility within the Biomedical Sciences Building at the University of Florida, where they were given free access to standard mouse chow (diet 2018S; Harlan Teklad) and water. For flux studies, male and female mice aged 2–5 months (20–30 g body mass) were killed by cervical dislocation following prior sedation induced by brief inhalation of isoflurane (≤15 sec). The entire lower portion of the intestinal tract (proximal ileum to distal colon) was then dissected out and placed in ice-cold buffer for immediate preparation for transport experiments. All animal experimentation was approved by the University of Florida Institutional Animal Care and Use Committee (IACUC) and performed in accordance with the National Institutes of Health "Guide for the Care and Use of Laboratory Animals."

Epithelial transport experiments

Unidirectional fluxes of oxalate and Cl^- were measured simultaneously under symmetrical, short-circuit conditions across pairs of intact, isolated tissues taken from the

distal ileum (4 cm length immediately proximal to the ileo-cecal valve) and distal colon (4 cm length immediately proximal to the peritoneal border and representing the lower 30% of the large intestine). After removing the outer connective tissue each segment was opened longitudinally along the mesenteric border to form a flat sheet. From each segment a pair of tissues were prepared with each one mounted on a slider (P2304; Physiologic Instruments, San Diego, CA), exposing a gross surface area of 0.3 cm^2, and secured into a modified Ussing chamber (P2300). The mucosal and serosal surfaces were bathed with 4 mL buffered saline and maintained at 37°C while being simultaneously gassed and stirred with the appropriate hydrated gas mixture (Table 1). Each individual preparation was continuously voltage clamped to 0 mV with an automatic voltage clamp (model VCCMC6, Physiologic Instruments, San Diego, CA).

To measure the transepithelial fluxes of oxalate and Cl^-, 0.27 μCi of ^{14}C-oxalate (specific activity 115 mCi/mmol), and 0.09 μCi of ^{36}Cl (specific activity 571 μCi/mmol) were added to either the mucosal or serosal chamber and which was then designated as the "hot side". The addition of ^{14}C-oxalate to the "hot side" required the respective addition of 0.9 μmol/l "cold" oxalate in the form of Na_2Ox to achieve a final concentration of 1.5 μmol/l oxalate. This was matched by 1.5 μmol/l Na_2Ox on the opposing "cold side". At 15 min intervals 1 mL samples were taken from the "cold side" to detect the appearance of these tracers, along with a recording of short-circuit current (μA) and open-circuit potential difference (mV). Each sample taken from the "cold side" was immediately replaced with 1 mL of warmed buffer. At the beginning and end of each experiment a 50 μL sample was taken from the "hot side" and used to calculate the specific activity (dpm/mmol) of each isotope. The activity of ^{14}C-oxalate and ^{36}Cl in all samples was determined by liquid scintillation spectrophotometry (Beckman LS6500, Beckman-Coulter, Fullerton, CA) with quench correction following dissolution in 5 mL scintillation cocktail (Ecoscint A, National Diagnostics, Atlanta, GA). Using a series of external standards for each isotope, the validity of counting dual-labeled samples was independently established thus allowing the individual activities of ^{14}C-oxalate and ^{36}Cl to be calculated on the basis of their relative counting efficiencies after modifying the detection channels to minimize overlap in their respective energy spectra.

The epithelial responses to the CA inhibitors, ethoxzolamide, and N-3500, as well as to increased CO_2 partial pressure (P_{CO_2}) were performed as part of a paired experimental design. This involved commencement of an initial "control" period (0–45 min; Period I), after which the

Table 1. The nominal concentration (mmol/L) of salts composing the buffers used in the following study. Each bicarbonate-containing buffer was equilibrated with a 95% O_2/5% CO_2 gas mixture at 37°C prior to measuring pH, total CO_2, and osmolality. To elevate P_{CO_2} in the standard, 21 mmol/L HCO_3^- buffer an 89% O_2/11% CO_2 mixture was used.

	Bicarbonate				Bicarbonate-free		
Salt	7 mmol/L	21 mmol/L	21 mmol/L (High CO_2)	42 mmol/L	pH 6.9	pH 7.4	pH 7.9
NaCl	118.4	118.4	118.4	97.4	118.4	118.4	118.4
K_2HPO4	2.4	2.4	2.4	2.4	2.4	2.4	2.4
KH_2PO4	0.6	0.6	0.6	0.6	0.6	0.6	0.6
$NaHCO_3$	7.0	21.0	21.0	42.0	–	–	–
$MgSO_4$	0.5	0.5	0.5	0.5	0.5	0.5	0.5
$CaCl_2$	1.2	1.2	1.2	1.2	1.2	1.2	1.2
$MgCl_2$	0.7	0.7	0.7	0.7	0.7	0.7	0.7
HEPES (free acid)	–	–	–	–	21.0	14.0	7.0
HEPES (Na^+-salt)	–	–	–	–	–	7.0	14.0
Na^+-gluconate	14	–	–	–	–	–	–
Mannitol	–	–	–	–	13	8	–
Gas mixture	95% O_2/5% CO_2	95% O_2/5% CO_2	89% O_2/11% CO_2	95% O_2/5% CO_2	100% O_2	100% O_2	100% O_2
pH at 37°C	6.993	7.460	7.135	7.745	6.761	7.261	7.736
P_{CO_2} at 37°C (mmHg)	29.6	28.0	64.0	30.6	–	–	–
Osmolality (mOsm/kg)	276	272	281	278	269	270	269

designated treatment was applied and the effects recorded for a further 60 min (45–105 min; Period II). In a bid to try and distinguish the involvement of intracellular CA isoforms (CAI and CAII) from the extracellular apical membrane-bound CAIV (Goldfarb et al. 2000), we utilized the impermeant CA inhibitor N-3500 (Delacruz et al. 2010). To target the external CAIV, N-3500 was added to the mucosal bath at the end of the initial control period (Period I). At the conclusion of Period II the membrane-permeant ethoxzolamide was then applied for a final third period (105–165 min; Period III) to inhibit all CA activity. The response to ethoxzolamide was tested in all buffers, whereas the effects of increasing P_{CO_2}, and the impact of N-3500 (coupled with ethoxzolamide) were examined in standard 21 mmol/L HCO_3^- buffer only. For each buffer shown in Table 1, the data collected during the initial control period of these paired experiments was subsequently used to independently compare the effects of varying $[HCO_3^-]$ and pH.

Buffer solutions and reagents

Table 1 displays the nominal salt composition and characteristics of each buffer. The standard bicarbonate buffer contained 21 mmol/L HCO_3^- and was gassed with 95% O_2/5% CO_2 to achieve a pH and P_{CO_2} of 7.4 and 28 mmHg, respectively. To reduce $[HCO_3^-]$ to 7 mmol/L, two-thirds of the $NaHCO_3$ was replaced with 14 mmol/L sodium gluconate, and to help limit the increase in osmolality when increasing $[HCO_3^-]$ to 42 mmol/L, the [NaCl] was reduced by 21 mmol/L. The $[HCO_3^-]$ and P_{CO_2} of each bicarbonate buffer was calculated following re-arrangement of the Henderson–Hasselbalch equation using measurements of pH and total CO_2 (tCO_2). pH was measured with an accupHast combination microelectrode (Fisher Scientific) connected to a Beckman 690 pH meter (Beckman-Coulter, Fullerton, CA), and tCO_2 by a Corning 965 CO_2 analyzer (Corning Ltd., Halstead, Essex, U.K.). To achieve a HCO_3^-/CO_2 free buffer $NaHCO_3$ was replaced with equimolar HEPES buffers and gassed with 100% O_2. To modify pH under these conditions the concentrations of these complementary HEPES buffers were modified accordingly and in some cases necessitated the addition of mannitol to preserve osmolality (Table 1). As part of this study was examining the effects of CA inhibition, the HCO_3^-/CO_2-free buffers did not include a CA inhibitor. In all cases, the serosal buffer contained 10 mmol/L glucose, with an equivalent 10 mmol/L mannitol included in each mucosal buffer. To inhibit endogenous prostanoid production all buffers contained 5 μmol/L indomethacin (Sigma, St. Louis, MO). The CA inhibitor ethoxzolamide was sourced from Sigma, and the 11% CO_2/89% O_2 gas mixture from Airgas Inc. A concentrated stock solution of ethoxzolamide in DMSO was made fresh on the day of each experiment and added to both mucosal and serosal chambers to a final concentration 100 μmol/L, the resulting amount of DMSO in each half chamber was 0.05%. The impermeant CA inhibitor N-3500 was custom synthesized (Delacruz et al. 2010) and dissolved in standard HCO_3^- buffer prior to addition to the mucosal bath at a final concentration of 100 μmol/L. The isotope ^{14}C-oxalate was a custom preparation from ViTrax Radiochemicals (Placentia, CA) and ^{36}Cl was purchased as HCl from Amersham Biosciences (Piscataway, NJ).

Calculations and statistical analyses

The $[HCO_3^-]$ and P_{CO_2} of each HCO_3^-/CO_2-containing buffer was calculated from the measurements of pH and tCO_2 (mmol/L) using the following re-arrangement of the Henderson–Hasselbalch equation: $[dCO_2] = [tCO_2]/(1 + 10\text{^}(pH-pK''(aq)))$, where dCO_2 is dissolved CO_2, (mmol/L), and pK″(aq) is the first dissociation constant for carbonic acid corrected for the ionic strength and pH of the aqueous buffer solution (Siggaard-Andersen 1974). For the standard bicarbonate buffer at 37°C pK″(aq) was 6.118. The $[HCO_3^-]$ (mmol/L) was subsequently calculated by: $[HCO_3^-] = [tCO_2] - [dCO_2]$, and P_{CO_2} (mmHg) by: $P_{CO_2} = [dCO_2]/\alpha$, where α is the solubility coefficient of CO_2 (0.032 mmol/L•mmHg), corrected for the ionic strength of the buffer (Siggaard-Andersen 1974).

The fluxes of oxalate and Cl^- in the absorptive, mucosal to serosal (J_{ms}^{ion}) and secretory, serosal to mucosal (J_{sm}^{ion}) directions were calculated from the change in activity of ^{14}C-oxalate or ^{36}Cl detected on the "cold side" of the chamber at each 15 min sampling point, having corrected for dilution with replacement buffer between samples. These flux rates were expressed per cm^2 of tissue surface area per hour. The recordings of short-circuit current (I_{sc}; μA) and transepithelial potential difference (mV) were used to calculate transepithelial conductance (G_t; mS/cm^2) following Ohm's Law. For each segment net fluxes (J_{net}^{ion}) were calculated as: $J_{net}^{ion} = J_{ms}^{ion} - J_{sm}^{ion}$ from tissues matched on the basis of conductance (no greater than a $\pm$ 15% difference in G_t between pairs of tissues from the distal ileum, and not exceeding $\pm$ 25% for tissue pairs from the distal colon).

The following data are presented as mean $\pm$ SE. For experiments conducted as a paired design, a repeated-measures, one-way ANOVA was used to evaluate the epithelial response to treatment with ethoxzolamide, 11% CO_2, or N-3500 followed by ethoxzolamide, at each subsequent 15 min time point compared to the preceding control period. This control period value was taken as the mean of data points collected between 0 and 45 min.

Significant differences following the experimental treatment were subsequently distinguished by multiple comparisons to the corresponding control value using Holm-Sidak post-hoc tests. Differences in flux rates and electrical characteristics in the presence of buffers with varying [HCO_3^-] or pH were assessed by one-way ANOVA followed by Holm–Sidak multiple pairwise comparisons. For data failing to meet the assumptions of approximate normality and equality of variance, the equivalent nonparametric tests were performed. The results of all statistical tests were accepted as significant at $P < 0.05$. Statistical analysis was performed with SigmaStat v3.5 and the figures drawn using SigmaPlot v11.0 (Systat Software Inc. San Jose, CA).

Results

Effects of varying [HCO_3^-]

Tables 2 and 3 show that in standard buffer (21 mmol/L HCO_3^-) the distal ileum and distal colon mediated net oxalate secretion. In Table 2, reducing extracellular [HCO_3^-] to 7 mmol/L or eliminating it altogether, did not significantly impact oxalate fluxes by the distal ileum. The latter condition, did result in net Cl^- secretion (-2.49 ± 1.24 μmol/cm^2/h), through a 30% decrease in J_{ms}^{Cl}. This indicates that even with CA activity intact, endogenous metabolic production of HCO_3^- was insufficient to sustain Cl^- absorption and was thus dependent on an extracellular supply of HCO_3^-/CO_2. In this segment of the lower small intestine, when [HCO_3^-] was increased to 42 mmol/L both oxalate and Cl^- fluxes were significantly affected cutting J_{sm}^{Ox} and J_{ms}^{Cl} by 45 and 24%, respectively, with no accompanying alterations to I_{sc} or G_t (Table 2). Conversely, in the distal colon (Table 3), eliminating HCO_3^-/CO_2 exclusively reduced J_{sm}^{Ox} by 28% consequently abolishing net oxalate secretion by this segment. The net secretion of oxalate was also greatly diminished at 42 mmol/L HCO_3^-, again through a decreased J_{sm}^{Ox} flux. Surprisingly, net Cl^- absorption was independent of [HCO_3^-], even in HEPES buffer where J_{ms}^{Cl} was not diminished, although J_{sm}^{Cl} was 25% higher (Table 3).

Effects of changing pH

The absence of HCO_3^- and CO_2 permitted buffer pH to be manipulated independently of these two variables. Under these circumstances pH did not exert any significant impacts on net oxalate or Cl^- transport for either segment examined. For the distal ileum, altering pH between 6.9 and 7.9 did produce a significant increase in I_{sc} from -1.70 to -4.22 μeq/cm^2/h, which was approxi-

Table 2. Effects of [HCO_3^-] on oxalate and chloride transport by the distal ileum. A comparison of transepithelial oxalate (J^{Ox}) and Cl^- (J^{Cl}) fluxes measured simultaneously during period I (0–45 min) in buffers containing different concentrations of HCO_3^- across pairs of isolated, short-circuited segments of the distal ileum from wild-type mice. Short-circuit current (I_{sc}) and transepithelial conductance (G_t) are also shown. Data are mean ± SE and values labeled with a different letter indicate a statistically significant difference. Numbers in parentheses denote sample size.

	J^{Ox} (pmol/cm^2/h)			J^{Cl} (μmol/cm^2/h)					
[HCO_3^-] (mmol/L)	J_{ms}	J_{sm}	J_{net}	J_{ms}	J_{sm}	J_{net}	I_{sc} (μeq/cm^2/h)	G_t (mS/cm^2)
0 (pH 7.4)	16.70 ± 2.17 (8)	52.39 ± 5.50^a (8)	−35.69 ± 6.78 (8)	7.80 ± 0.65^a (8)	10.28 ± 1.15 (8)	−2.49 ± 1.24^a (8)	−1.95 ± 0.26 (16)	25.84 ± 1.81 (16)
7 (pH 6.9)	22.36 ± 5.74 (5)	56.35 ± 7.70^a (5)	−33.99 ± 5.64 (5)	11.01 ± 1.25^{a,b} (5)	10.19 ± 1.49 (5)	0.82 ± 1.23^{a,b} (5)	−3.37 ± 0.61 (10)	32.40 ± 3.90 (10)
21 (pH 7.4)	27.39 ± 3.69 (24)	52.26 ± 3.24^a (24)	−24.87 ± 4.78 (24)	11.16 ± 0.49^b (24)	9.43 ± 0.45 (24)	1.72 ± 0.62^b (24)	−2.49 ± 0.17 (56)	29.05 ± 0.98 (56)
42 (pH 7.9)	19.81 ± 3.55 (5)	28.99 ± 3.77^b (5)	−9.18 ± 5.70 (5)	8.45 ± 0.42^{a,b} (5)	8.49 ± 1.00 (5)	−0.04 ± 1.13^{a,b} (5)	−2.62 ± 0.36 (10)	31.43 ± 2.03 (10)

Table 3. Effects of $[HCO_3^-]$ on oxalate and chloride transport by the distal colon. A comparison of transepithelial oxalate (J^{Ox}) and Cl^- (J^{Cl}) fluxes measured simultaneously during period I (0–45 min) in buffers containing different concentrations of HCO_3^- across pairs of isolated, short-circuited segments of the distal colon from wild-type mice. Short-circuit current (I_{sc}) and transepithelial conductance (G_t) are also shown. Data are mean ± SE and values labeled with a different letter indicate a statistically significant difference. Numbers in parentheses denote associated sample size.

$[HCO_3^-]$ (mmol/L)	J^{Ox} (pmol/cm²/h)			J^{Cl} (μmol/cm²/h)			I_{sc} (μeq/cm²/h)	G_t (mS/cm²)
	J_{ms}	J_{sm}	J_{net}	J_{ms}	J_{sm}	J_{net}		
0 (pH 7.4)	26.16 ± 1.75^{a,b} (12)	26.58 ± 2.98^{a} (12)	−0.42 ± 2.96^{a} (12)	16.51 ± 1.06 (8)	14.85 ± 0.95^{a} (8)	1.66 ± 1.38 (8)	−0.29 ± 0.12^{a} (24)	10.45 ± 0.74^{a} (24)
7 (pH 6.9)	27.54 ± 2.72^{a} (11)	37.43 ± 1.81^{b} (11)	−9.89 ± 3.25^{a,b} (11)	15.58 ± 0.75 (8)	11.85 ± 0.32^{b} (8)	3.74 ± 0.80 (8)	−0.53 ± 0.11^{a,b} (20)	11.52 ± 0.77^{a,b} (20)
21 (pH 7.4)	20.75 ± 1.27^{b} (24)	36.70 ± 1.55^{b} (24)	−15.95 ± 1.56^{b} (24)	15.80 ± 0.58 (20)	11.84 ± 0.35^{b} (20)	3.96 ± 0.69 (20)	−0.67 ± 0.07^{b} (54)	13.55 ± 0.63^{b} (54)
42 (pH 7.9)	17.51 ± 2.57^{b} (6)	20.33 ± 1.71^{a} (6)	−2.81 ± 1.94^{a} (6)	13.94 ± 1.28 (6)	12.57 ± 0.87^{a,b} (6)	1.37 ± 1.86 (6)	−1.18 ± 0.15^{c} (12)	11.99 ± 0.72^{a,b} (12)

mately equivalent in magnitude to the resulting net Cl^- secretion at pH 7.9 (5.38 ± 1.67 μmol/cm²/h). In addition, this higher pH also produced an increase in G_t (Table 4). Even though the absence of HCO_3^- and CO_2 abolished net oxalate secretion by the distal colon, changing pH under these circumstances did not produce any other dramatic effects on oxalate fluxes by this segment, although J_{ms}^{Cl} was significantly lower at pH 7.9 this did not translate to a significant change in net Cl^- flux (Table 5).

Effect of increasing P_{CO_2}

There were no significant effects of increasing P_{CO_2} on oxalate or Cl^- fluxes across the distal ileum aside from a reduction in G_t (Fig. 1). In contrast, 11% CO_2 produced a clear, rapid increase in the secretory flux of oxalate by the distal colon (Fig. 2A) which translated to a significant 41% enhancement of net oxalate secretion from −17.50 ± 3.26 to −24.60 ± 3.13 pmol/cm²/h. There were, however, no accompanying changes to Cl^- fluxes (Fig. 2B), although I_{sc} gradually became positive (Fig. 2C).

Role of carbonic anhydrase

In Figure 3, application of the CA inhibitor ethoxzolamide did not impact any parameter in the distal ileum, with the exception of G_t which showed a very modest reduction (Fig. 3C). For the distal colon, there were dramatic changes to oxalate fluxes in response to CA inhibition, where net secretion was completely abolished (Fig. 4A). This was primarily through a 27% reduction in J_{sm}^{Ox}, with a smaller rise in J_{ms}^{Ox}. There was also an exclusive decrease in J_{ms}^{Cl}, lowering net Cl^- absorption by 60% (Fig. 4B), accompanied by a modest, but significant change in direction of I_{sc} (Fig. 4C). Targeting the external CA at the apical membrane of the distal colon with N-3500 did not significantly diminish J_{sm}^{Ox}, only the subsequent addition of ethoxzolamide was able to inhibit net oxalate secretion (Fig. 5A). Similarly, this final maneuver also abolished net Cl^- absorption via J_{ms}^{Cl}, where N-3500 had previously no effect (Fig. 5B), and was accompanied by an increasingly positive I_{sc} (Fig. 5C).

When ethoxzolamide was used to inhibit CA in the absence of extracellular HCO_3^-/CO_2, the distal ileum proved itself refractory to this maneuver also, with no significant effects on oxalate or Cl^- transport (Fig. 6A and B), although there was a transient increase in I_{sc} (Fig. 6C). The absence of net oxalate secretion by the distal colon under HCO_3^-/CO_2-free conditions did not change following the application of ethoxzolamide with no subsequent effect on unidirectional fluxes (Fig. 7A).

Table 4. Effects of pH on oxalate and chloride transport by the distal ileum. A comparison of transepithelial oxalate (J^{Ox}) and Cl^- (J^{Cl}) fluxes measured simultaneously during period I (0–45 min) in HCO_3^-/CO_2-free buffers of different pH across pairs of isolated, short-circuited segments of the distal ileum from wild-type mice. Short-circuit current (I_{sc}) and transepithelial conductance (G_t) are also shown. Data are mean ± SE and values labeled with a different letter indicate a statistically significant difference. Numbers in parentheses denote associated sample size.

	J^{Ox} (pmol/cm^2/h)			J^{Cl} (μmol/cm^2/h)				
pH	J_{ms}	J_{sm}	J_{net}	J_{ms}	J_{sm}	J_{net}	I_{sc} (μeq/cm^2/h)	G_t (mS/cm^2)
6.9	16.77 ± 1.80 (6)	50.71 ± 7.12 (6)	−33.94 ± 7.70 (6)	7.79 ± 0.37 (6)	9.08 ± 1.45 (6)	−1.28 ± 1.75 (6)	−1.70 ± 0.55^a (12)	23.91 ± 1.33^a (12)
7.4	16.70 ± 2.17 (8)	52.39 ± 5.50 (8)	−35.69 ± 6.78 (8)	7.80 ± 0.65 (8)	10.28 ± 1.15 (8)	−2.49 ± 1.24 (8)	−1.95 ± 0.26^a (16)	25.84 ± 1.81^a (16)
7.9	21.98 ± 2.76 (5)	51.07 ± 9.55 (5)	−29.09 ± 9.43 (5)	8.17 ± 0.65 (5)	13.55 ± 1.74 (5)	−5.38 ± 1.67 (5)	−4.22 ± 0.52^b (10)	32.55 ± 2.28^b (10)

Table 5. Effects of pH on oxalate and chloride transport by the distal colon. A comparison of transepithelial oxalate (J^{Ox}) and Cl^- (J^{Cl}) fluxes measured simultaneously during period I (0–45 min) in HCO_3^-/CO_2-free buffers of different pH across pairs of isolated, short-circuited segments of the distal colon from wild-type mice. Short-circuit current (I_{sc}) and transepithelial conductance (G_t) are also shown. Data are mean ± SE and values labeled with a different letter indicate a statistically significant difference. Numbers in parentheses denote associated sample size.

	J^{Ox} (pmol/cm^2/h)			J^{Cl} (μmol/cm^2/h)				
pH	J_{ms}	J_{sm}	J_{net}	J_{ms}	J_{sm}	J_{net}	I_{sc} (μeq/cm^2/h)	G_t (mS/cm^2)
6.9	27.88 ± 3.77 (6)	30.27 ± 4.47 (6)	−2.38 ± 4.60 (6)	15.69 ± 0.80^{a,b} (6)	14.10 ± 0.61 (6)	1.59 ± 1.08 (6)	−0.66 ± 0.25 (12)	12.09 ± 1.03 (12)
7.4	26.16 ± 1.75 (12)	26.58 ± 2.98 (12)	−0.42 ± 2.96 (12)	16.51 ± 1.06^a (8)	14.85 ± 0.95 (8)	1.66 ± 1.38 (8)	−0.29 ± 0.12 (24)	10.45 ± 0.74 (24)
7.9	20.25 ± 3.18 (8)	22.75 ± 2.58 (8)	−2.26 ± 4.07 (8)	12.23 ± 1.06^b (8)	12.79 ± 0.73 (8)	−0.55 ± 1.55 (8)	−0.69 ± 0.21 (16)	12.61 ± 0.91 (16)

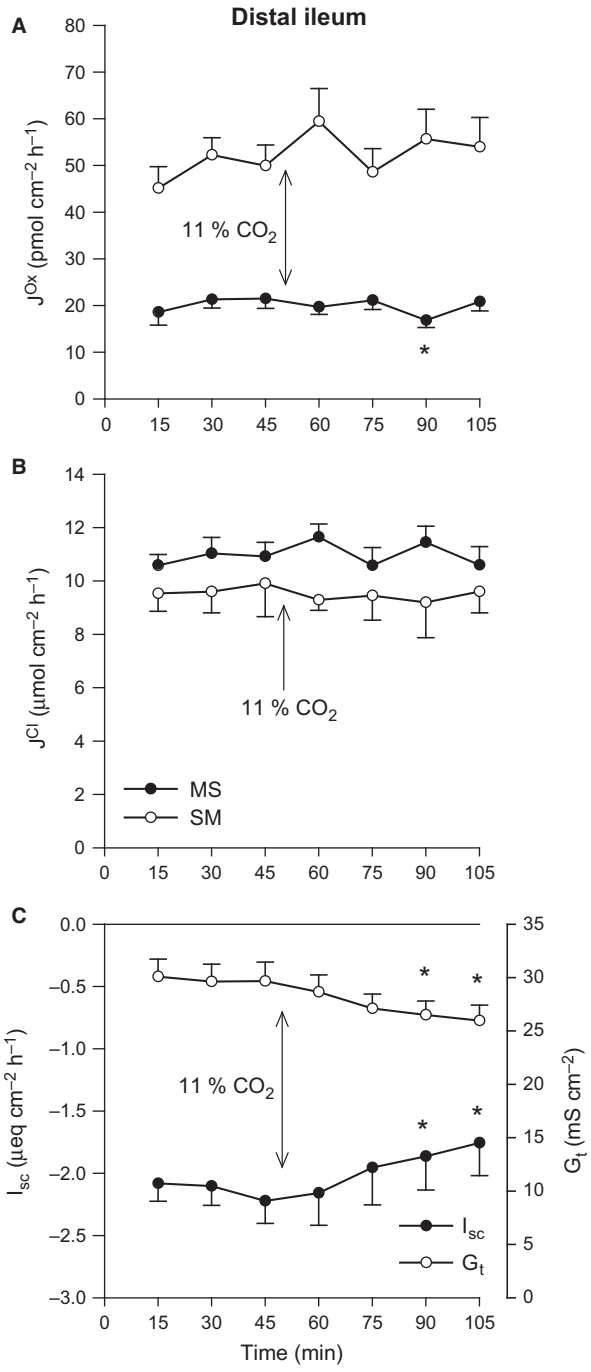

Figure 1. Effects of elevated P_{CO_2} on oxalate and chloride transport by the distal ileum. The unidirectional oxalate fluxes, J^{Ox} (pmol/cm^2/h), and Cl^- fluxes, J^{Cl} (μmol/cm^2/h), measured across isolated, short-circuited segments of distal ileum in standard bicarbonate buffer following an increase in P_{CO_2} using 11% CO_2 (mucosal + serosal), are shown in Panels A and B, respectively. Panel C displays the responses of short-circuit current (I_{sc}) and transepithelial conductance (G_t). Each data point represents mean ± SE of tissue pairs from n = 8 wild-type mice. An asterisk represents a statistically significant change from the preceding control period (0–45 min).

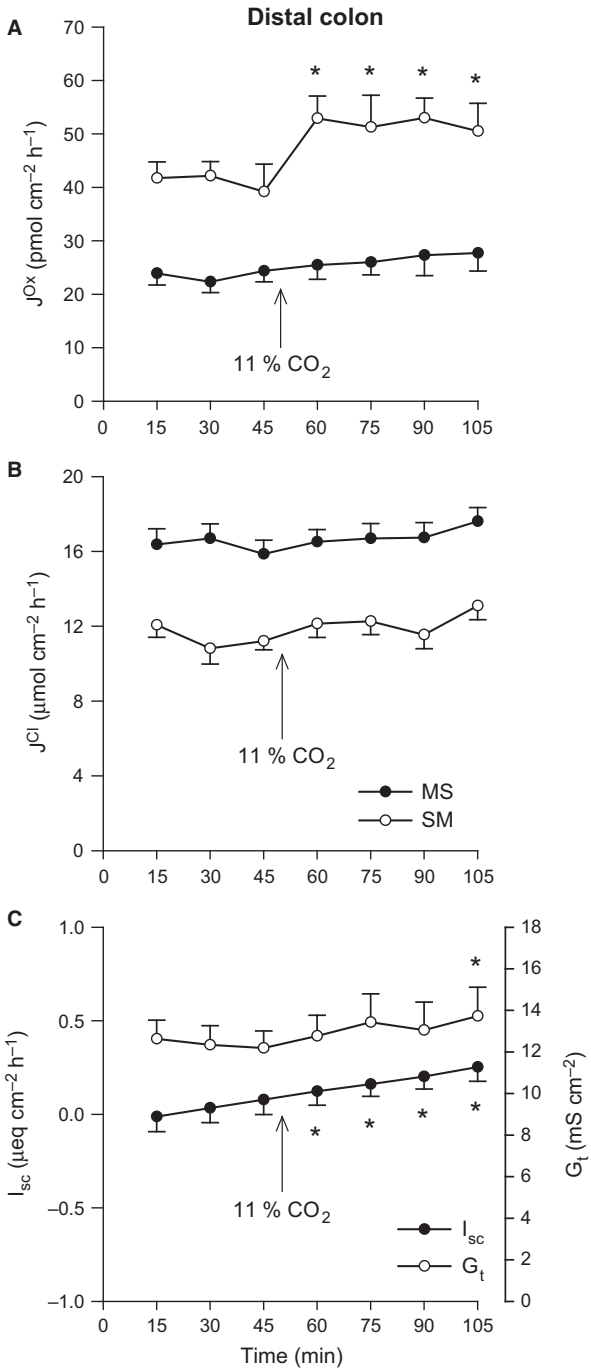

Figure 2. Effects of elevated P_{CO_2} on oxalate and chloride transport by the distal colon. The unidirectional oxalate fluxes, J^{Ox} (pmol/cm^2/h), and Cl^- fluxes, J^{Cl} (μmol/cm^2/h), measured across isolated, short-circuited segments of distal colon in standard bicarbonate buffer following an increase in P_{CO_2} using 11% CO_2 (mucosal + serosal), are shown in Panels A and B, respectively. Panel C displays the responses of short-circuit current (I_{sc}) and transepithelial conductance (G_t). Each data point represents mean ± SE of tissue pairs from n = 8 wild-type mice. An asterisk represents a statistically significant change from the preceding control period (0–45 min).

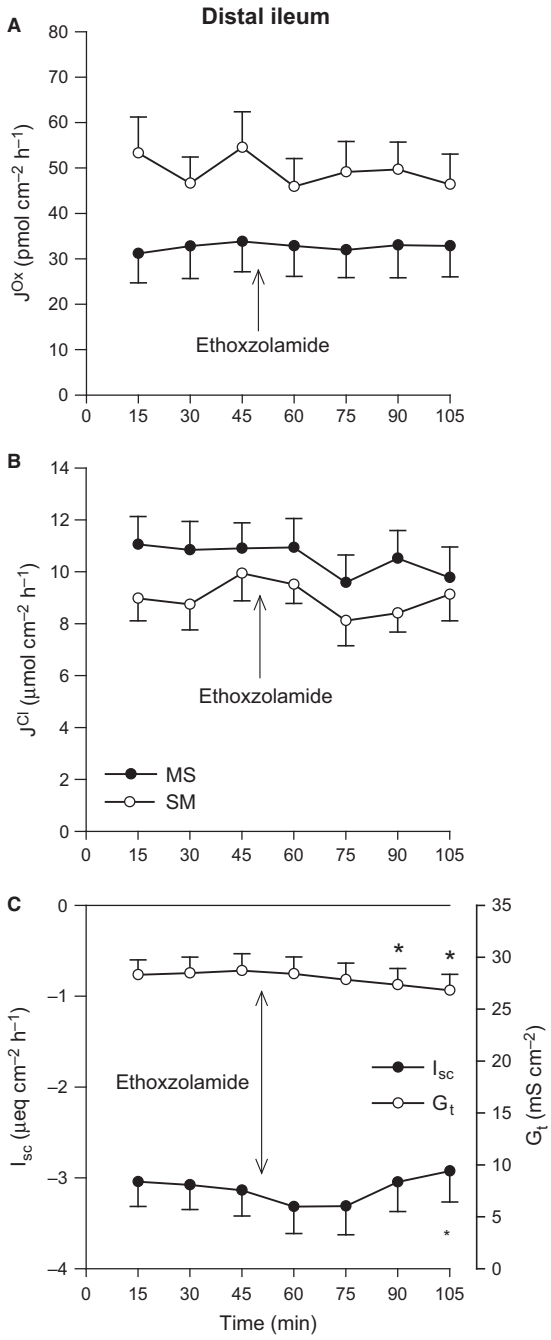

Figure 3. Effects of carbonic anhydrase inhibition on oxalate and chloride transport by the distal ileum. The unidirectional oxalate fluxes, J^{Ox} (pmol/cm^2/h), and Cl^- fluxes, J^{Cl} (μmol/cm^2/h), measured across isolated, short-circuited segments of distal ileum in standard bicarbonate buffer following application of the carbonic anhydrase inhibitor ethoxzolamide (100 μmol/L, mucosal + serosal), are shown in Panels A and B, respectively. Panel C displays the responses of short-circuit current (I_{sc}) and transepithelial conductance (G_t). Each data point represents mean ± SE of tissue pairs from n = 15 wild-type mice. An asterisk represents a statistically significant change from the preceding control period (0–45 min).

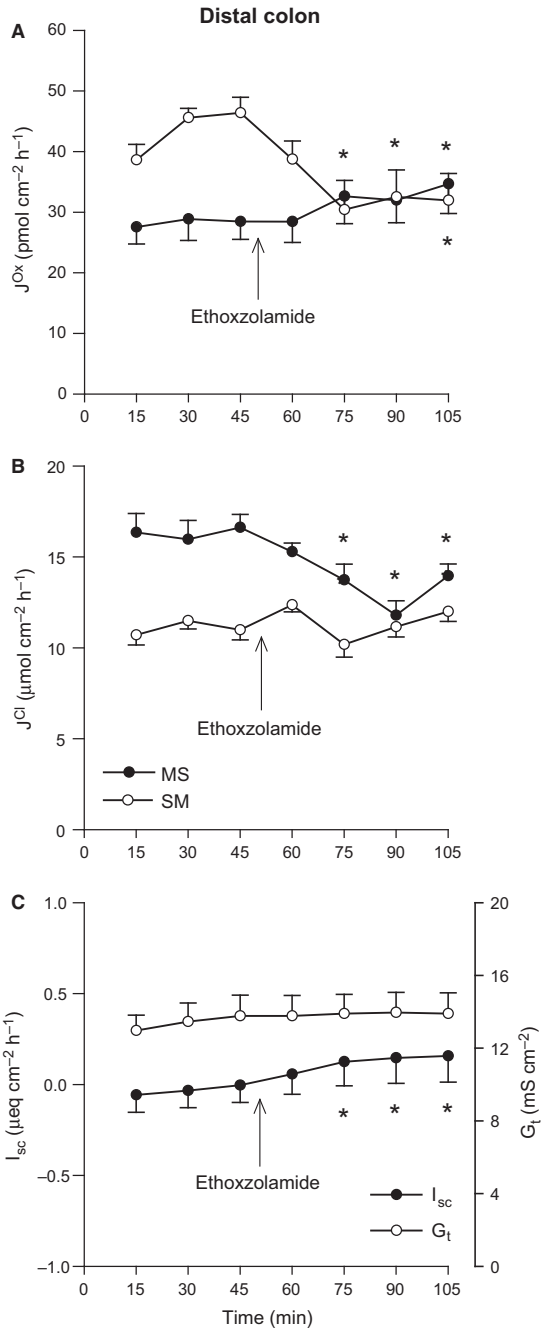

Figure 4. Effects of carbonic anhydrase inhibition on oxalate and chloride transport by the distal colon. The unidirectional oxalate fluxes, J^{Ox} (pmol/cm^2/h), and Cl^- fluxes, J^{Cl} (μmol/cm^2/h), measured across isolated, short-circuited segments of distal colon in standard bicarbonate buffer following application of the carbonic anhydrase inhibitor ethoxzolamide (100 μmol/L, mucosal + serosal), are shown in Panels A and B, respectively. Panel C displays the responses of short-circuit current (I_{sc}) and transepithelial conductance (G_t). Each data point represents mean ± SE of tissue pairs from n = 8 wild-type mice. An asterisk represents a statistically significant change from the preceding control period (0–45 min).

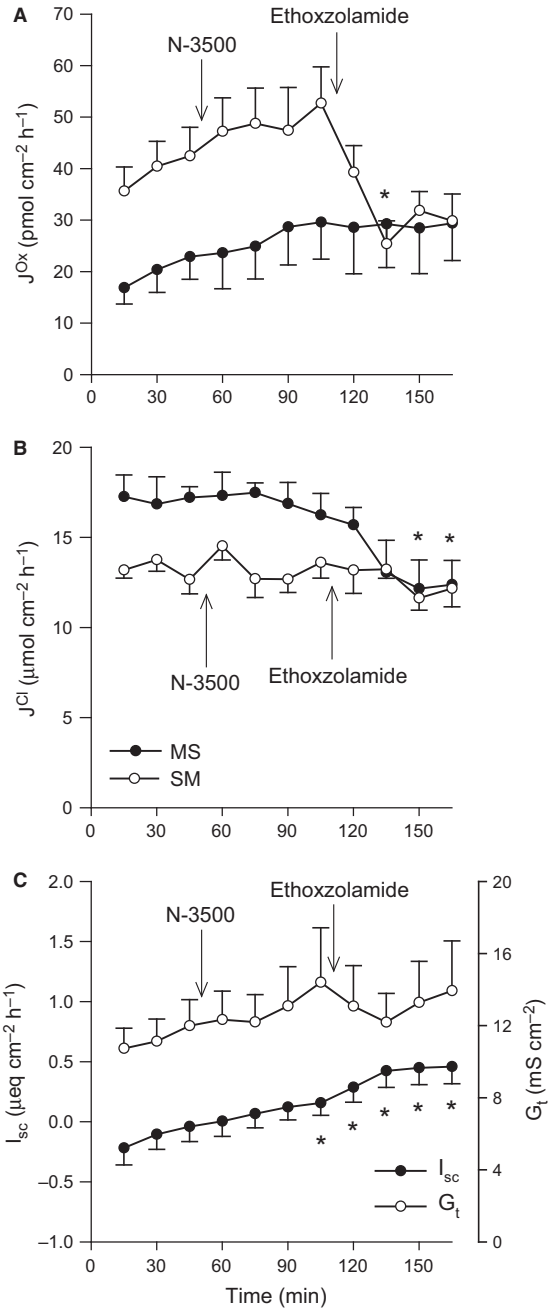

Figure 5. Effects of carbonic anhydrase inhibition on oxalate and chloride transport by the distal colon. The unidirectional oxalate fluxes, J^{Ox} (pmol/cm^2/h), and Cl^- fluxes, J^{Cl} (μmol/cm^2/h), measured across isolated, short-circuited segments of distal colon in standard bicarbonate buffer following application of the membrane-impermeant carbonic anhydrase inhibitor N-3500 (100 μmol/L, mucosal only), followed by ethoxzolamide (100 μmol/L, mucosal + serosal), are shown in Panels A and B, respectively. Panel C displays the responses of short-circuit current (I_{sc}) and transepithelial conductance (G_t). Each data point represents mean ± SE of tissue pairs from n = 6 wild-type mice. An asterisk represents a statistically significant change from the preceding control period (0–45 min).

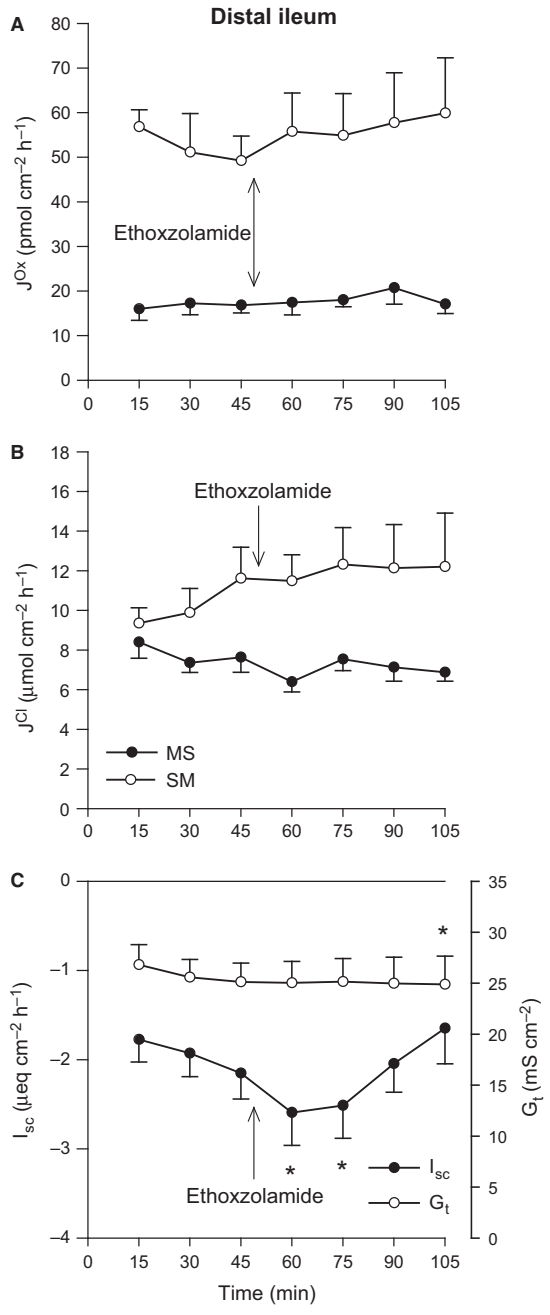

Figure 6. Effects of carbonic anhydrase inhibition on oxalate and chloride fluxes by the distal ileum in HEPES buffer. The unidirectional oxalate fluxes, J^{Ox} (pmol/cm^2/h), and Cl^- fluxes, J^{Cl} (μmol/cm^2/h), measured across isolated, short-circuited segments of distal ileum in HCO_3^-/CO_2-free HEPES buffer following application of the carbonic anhydrase inhibitor ethoxzolamide (100 μmol/L, mucosal + serosal), are shown in Panels A and B, respectively. Panel C displays the responses of short-circuit current (I_{sc}) and transepithelial conductance (G_t). Each data point represents mean ± SE of tissue pairs from n = 8 wild-type mice. An asterisk represents a statistically significant change from the preceding control period (0–45 min).

The reduction in J_{ms}^{Cl} seen previously with CA inhibition in standard HCO_3^- buffer was also evident in HEPES buffer and eliminated net Cl^- absorption (Fig. 7B).

Discussion

Previous work comprehensively established that states of acute respiratory and metabolic acidosis or alkalosis produce rapid, reversible alterations to NaCl absorption, HCO_3^- secretion and fluid handling by the ileum and colon in vivo. These effects were subsequently shown to be specific responses by the apical Na^+/H^+ and Cl^-/HCO_3^- exchangers to extracellular HCO_3^- concentration ($[HCO_3^-]_e$), P_{CO_2} and pH, through corresponding alterations to intracellular pH (pH_i) and HCO_3^- ($[HCO_3^-]_i$), mediated by CA. As oxalate is a substrate of the intestinal Cl^-/HCO_3^- exchangers, the aim of this study was to systematically examine how these acid-base variables impacted oxalate transport by the mouse intestine in vitro. Under standard buffer conditions we found the distal ileum and distal colon each mediated net oxalate secretion and Cl^- absorption, but only the latter segment and notably the J_{sm}^{Ox} pathway, were exclusively responsive to changes in $HCO_3^-{}_e$, P_{CO_2} and dependent on CA activity. Oxalate secretion, but not Cl^- absorption, by the distal colon was acutely stimulated by increasing P_{CO_2}. These findings highlight the distinct segmental heterogeneity of oxalate transport in the intestine, provide important new insights into the characteristics of the transport mechanism, and strongly imply that oxalate secretion by the mouse distal colon is specifically regulated by CO_2.

Effects of acid-base variables on Cl^- transport by the mouse intestine

The responses of intestinal Na^+ and Cl^- transport to pH, HCO_3^- and CO_2, and the role of CA, have been studied extensively in the rat model, and to a lesser degree in the mouse. As this was the first study investigating the relationship between oxalate and these acid-base variables in the mouse, simultaneously measuring Cl^- fluxes provided important points of reference to these earlier investigations and assisted subsequent interpretation of the associated oxalate fluxes. Net Cl^- absorption by the rat distal ileum in vivo, and specifically J_{ms}^{Cl} in vitro, was indirectly proportional to extracellular pH, whether produced by alterations in P_{CO_2}, $[HCO_3^-]_e$ or in HCO_3^-/CO_2-free HEPES buffer (Charney and Feldman 1984; Kurtin and Charney 1984; Wagner et al. 1986; Vaccarezza and Charney 1988; Charney et al. 1991), and also dependent on CA (Charney et al. 1986, 2002a). Subsequent work on this segment in the mouse showed that increasing P_{CO_2} from 21 to 70 mmHg stimulated net Cl^- absorption in identi-

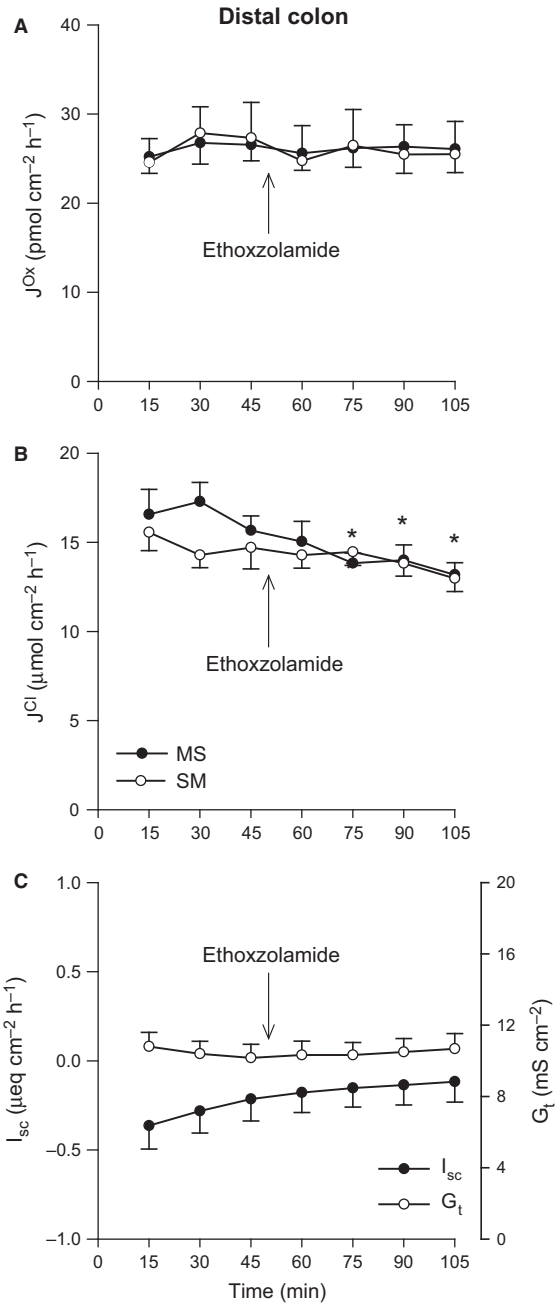

Figure 7. Effects of carbonic anhydrase inhibition on oxalate and chloride fluxes by the distal colon in HEPES buffer. The unidirectional oxalate fluxes, J^{Ox} (pmol/cm^2/h), and Cl^- fluxes, J^{Cl} (μmol/cm^2/h), measured across isolated, short-circuited segments of distal colon in HCO_3^-/CO_2-free HEPES buffer following application of the carbonic anhydrase inhibitor ethoxzolamide (100 μmol/L, mucosal + serosal), are shown in Panels A and B, respectively. Panel C displays the responses of short-circuit current (I_{sc}) and transepithelial conductance (G_t). Each data point represents mean ± SE of tissue pairs from n = 12 wild-type mice. An asterisk represents a statistically significant change from the preceding control period (0–45 min).

cal fashion (Charney et al. 2004b). In contrast, we found ileal Cl^- fluxes were unresponsive when subjected to a similar elevation of P_{CO_2} (Fig. 1B). Reducing pH from 7.61 to 7.09 in HEPES buffer stimulated J_{ms}^{Cl} by the rat ileum 16% (Vaccarezza and Charney 1988), yet we found Cl^- fluxes by the mouse ileum were not significantly altered between pH 6.9 and 7.9 (Table 4). The absence of HCO_3^-/CO_2 reversed net Cl^- absorption to net secretion exclusively through a reduction in J_{ms}^{Cl} (Table 2), indicating endogenous HCO_3^- production was insufficient to support apical Cl^-/HCO_3^- exchange and was thus dependent on HCO_3^- supplied from the serosal bath. This notion was corroborated by the inability of CA inhibitor ethoxzolamide to impact Cl^- fluxes (Figs. 3B and 5B), and consistent with the abolition of DIDS-sensitive (mucosal Cl^--dependent) HCO_3^- secretion by the mouse distal ileum following the removal of serosal HCO_3^-/CO_2 (Uchiyama et al. 2007; Zhang et al. 2007). A role for CA in the mouse ileum cannot be dismissed entirely as Uchiyama et al. (2007) observed that Cl^--dependent HCO_3^- secretion was reduced ~ 30% in the presence of 100 μmol/L acetazolamide. In contrast, net Cl^- absorption by the rat ileum was sustained in the absence of HCO_3^-/CO_2 (Vaccarezza and Charney 1988), and furthermore was sensitive to methazolamide (Charney et al. 2002a), indicating a prominent contribution of CA to ileal transport.

These acid-base variables also exert their effects on Na^+ and Cl^- absorption by the rat distal colon in vitro in a similar manner (Goldfarb et al. 1988), a segment characterized as sensitive to CO_2 rather than pH (Charney and Dagher 1996; Charney et al. 2004a). Subsequent work on the mouse distal colon in vitro revealed trends largely consistent with the rat, where raising P_{CO_2} to 69 mmHg exclusively stimulated J_{ms}^{Cl} (Goldfarb et al. 2000; Charney et al. 2004b), while reducing pH from 7.61 to 7.09 (in HEPES buffer) notably enhanced net Cl^- absorption through a reduction in J_{sm}^{Cl} (Goldfarb et al. 2000). Unlike these previous studies, we found increasing P_{CO_2} did not stimulate Cl^- fluxes by the distal colon (Fig. 2B), and net Cl^- absorption was also independent of pH (Table 4). In the absence of HCO_3^-/CO_2 (pH 7.6), net Cl^- absorption in the rat and mouse distal colon was abolished due to a reduction of J_{ms}^{Cl}, relative to standard 21 mmol/L HCO_3^- buffer (Goldfarb et al. 1988, 2000; Charney et al. 2004a), indicating a limited contribution from metabolic HCO_3^- production. Conversely, Table 2 shows J_{ms}^{Cl} and J_{net}^{Cl}, were independent of HCO_3^-/CO_2, although interestingly the secretory J_{sm}^{Cl} flux was significantly higher in this HEPES buffer (discussed further on). In our study, $HCO_{3\,i}^-$ was therefore sufficient to maintain apical Cl^-/HCO_3^- exchange (represented by J_{ms}^{Cl}), in the absence of external HCO_3^-/CO_2, thus implying a substantial contribution from CA. This is supported by the observation that on average, ethoxzolamide reduced J_{ms}^{Cl} by a similar magnitude (~ 3–4 μmol/cm^2/h) whether HCO_3^-/CO_2 was present (Fig. 4B and 5B) or not (Fig. 6B). However, if CA is providing $HCO_{3\,i}^-$ from CO_2 to drive apical Cl^-/HCO_3^- exchange, then it is curious as to why increasing P_{CO_2} failed to stimulate J_{ms}^{Cl} (Fig. 2B) as shown reproducibly in previous studies, particularly as $[HCO_3^-]_i$ increases from 11.3 to 18.3 mmol/L when P_{CO_2} is raised from 21 to 69 mmHg (Dagher et al. 1992).

The reasons for the above discrepancies between our present work on the mouse and previous results are not clear. In relation to studies with rats, species-specific differences in the functional expression of the Cl^- transporter(s), particularly the anion exchanger, AE1 (Slc4a1), may be one explanation. Both DRA and AE1 are present in the rat colon (Rajendran et al. 2000), where they are suggested to operate as respective Cl^-/OH^- and Cl^-/HCO_3^- exchangers at the apical membrane, thus endowing AE1 as the principal Cl^- transporter (Rajendran and Binder 1999, 2000). This is significant considering the CO_2-stimulated increase in J_{ms}^{Cl} by the rat distal colon correlated with enhanced AE1 expression (Charney et al. 2004a). In contrast to a prominent role for AE1 in the rat large intestine, there is no evidence that this is the case for the mouse. Utilizing immunocytochemistry, Alper et al. (1999) found that antibodies directed against AE1 did not stain enterocytes from the mouse colon, and thus lacks AE1 expression. Although we note that more recent work has detected AE1 mRNA in the mouse large intestine (Gawenis et al. 2010). If AE1 is absent from the mouse intestine this might explain why increasing CO_2 failed to stimulate Cl^- absorption in this study. For the mouse (and human) intestine, DRA rather than AE1 has become recognized as the main Cl^-/HCO_3^- exchanger (Hoglund et al. 1996; Schweinfest et al. 2006; Kato and Romero 2011; Freel et al. 2013). Qualitatively, the mouse and rat share a near-identical pattern of DRA expression along the large intestine (Talbot and Lytle 2010), yet the relative contributions of DRA and AE1 to Cl^- transport for the latter model remain undetermined. In addition to species-specific differences, our data also showed similar departures from other mouse studies (Goldfarb et al. 2000; Charney et al. 2004b). As strain-related differences in intestinal transport do exist between mice this might offer some explanation. For example, duodenal calcium and phosphate absorption by C57BL/6 mice were found to be different from C3H/He mice (Armbrecht et al. 2002), whereas the stimulation of colonic ion secretion in Sv129 mice was distinct from the C57BL strain (Flores et al. 2010). For both of these studies the disparities between strains were, in part, the result of differences in respective transporter expression. A similar scenario, per-

haps related to functional AE1 expression, may explain why Cl^- absorption by the ileum and colon of the Balb/C mouse used by Charney et al. (2004b) responded to P_{CO_2}, but the C57BL/6 strain used here did not. We note that AE1 expression was absent from the large intestine of CD1 mice (Alper et al. 1999), whereas AE1 mRNA was detected in the colon of mice on a mixed 129SvEv/Black Swiss background (Gawenis et al. 2010). However, this line of reasoning becomes somewhat uncertain in relation to the findings of Goldfarb et al. (2000), who presented data pooled from C57BL/6J and DBA/2J mice, based on no measurable differences in Na^+ and Cl^- flux rates, CA isozyme expression or CA activity between strains.

Oxalate secretion by the distal colon is stimulated by CO_2

Although elevated P_{CO_2} unexpectedly failed to stimulate J^{Cl}_{ms}, it dramatically enhanced oxalate secretion (Fig. 2A). A major portion (70–75%) of CO_2-stimulated NaCl absorption by the rat distal colon corresponds to the CA-dependent trafficking of NHE3 and the anion exchanger AE1 (Slc4a1) to the apical membrane (Charney et al. 2002b, 2004a). As J^{Ox}_{sm} was also acutely stimulated by CO_2 (Fig. 2A), and dependent on CA (Fig. 4A), independent of any changes in G_t (Figs. 2C and 4C), we considered whether alterations to membrane transporter expression might also explain this response. If this increase in J^{Ox}_{sm} was due to changes in an apical Cl^-/HCO_3^- exchanger such as AE1 or DRA, then we would anticipate an accompanying increase in J^{Cl}_{ms}, but this was not the case (Fig. 2B). Furthermore, while DRA accounts for 50% of J^{Cl}_{ms} in the mouse distal colon, we have shown that it is involved in transcellular oxalate absorption rather than secretion (Freel et al. 2013), and notably P_{CO_2} was also without effect on J^{Ox}_{ms} (Fig. 2A). While PAT1 has been identified as the apical anion exchanger responsible for oxalate secretion by the small intestine (Freel et al. 2006; Jiang et al. 2006), the apical transporter(s) involved in the large intestine have not been resolved. Considered to be most prominent in the small intestine, PAT1 expression does extend into the large intestine (Wang et al. 2002; Hatch et al. 2011), yet its function there is uncertain. We have recently shown PAT1 contributes to sulfate (SO_4^{2-}) secretion by the mouse cecum (Whittamore et al. 2013), but whether this also applies to oxalate and the distal colon has yet to be revealed. Interestingly, PAT1 is considered responsive to systemic acid-base status, as PAT1-mediated HCO_3^- secretion by the mouse duodenum in vivo was decreased when the systemic acidosis induced by isoflurane anesthesia was left uncorrected (Singh et al. 2008). Although PAT1 contributes to J^{Ox}_{sm} in the distal ileum (Freel et al. 2006), we have shown here that oxalate secretion by this same segment was unaffected when subjected to acidotic conditions in vitro, that is, where $[HCO_3^-] = 7$ mmol/L and pH 6.9 (Table 3), and following an increase in P_{CO_2} (Fig. 1A). Previous work on the rabbit distal colon showed that J^{Ox}_{sm} and net oxalate secretion could be stimulated by cAMP with characteristics bearing resemblance to electrogenic Cl^- secretion (Hatch et al. 1994). Notably, CO_2 can elicit cAMP production by recombinant mammalian transmembrane adenylyl cyclases (tmACs) with an EC_{50} of ~2 mmol/L (Townsend et al. 2009), which is similar to the $[CO_2]$ achieved with 11% CO_2 here (2.1 mmol/L). In contrast, CO_2-stimulated oxalate secretion by the mouse distal colon appeared to be independent of a cAMP-mediated pathway, as Cl^- fluxes (Fig. 4B) and I_{sc} (Fig. 4C) indicated no substantial induction of Cl^- or HCO_3^- secretion. Furthermore, the application of 10 μmol/L forskolin (a potent agonist of the tmACs) does not stimulate oxalate secretion by the mouse distal colon (Whittamore, J. M. and Hatch, M., unpublished observations).

Intracellular bicarbonate mediates changes to intestinal ion transport

A common factor linking previous studies on the regulation of intestinal Cl^- transport to our present observations on oxalate, and to some extent Cl^- fluxes, is $[HCO_3^-]_i$. We found J^{Ox}_{sm} was exclusively sensitive to changes in $[HCO_3^-]_e$ and P_{CO_2}, maneuvers that each result in proportional changes to $[HCO_3^-]_i$. Every 1 mmol/L increase in $[HCO_3^-]_e$ at a constant P_{CO_2} (32 mmHg) has been determined to produce a corresponding 0.54 mmol/L increase in $[HCO_3^-]_i$, while every 1 mmHg rise in P_{CO_2} increases $[HCO_3^-]_i$ by 0.12 mmol/L (Dagher et al. 1992). In the rat distal colon $[HCO_3^-]_i$ modulates basal and carbachol-stimulated Cl^- secretion (Dagher et al. 1992, 1994), where J^{Cl}_{sm} was inversely related to $[HCO_3^-]_i$ above or below a physiological "plateau" of 9–18 mmol/L (Dagher et al. 1992). We too observed that J^{Ox}_{sm} conferred net oxalate secretion between 7 and 21 mmol/L HCO_3^- (Table 3), and J^{Ox}_{sm} could be stimulated by increasing P_{CO_2} (Fig. 2A), corresponding to an estimated $[HCO_3^-]_i$ within a very similar range of 8–20 mmol/L. Either side of this range J^{Ox}_{sm} was reduced and net oxalate secretion abolished (Table 3). Lowering $[HCO_3^-]_e$ from 21 mmol/L to zero at pH 7.4 increased J^{Cl}_{sm} by the rat distal colon 65%, from 7.9 to 13.0 μmol/cm^2/h (Dagher et al. 1992). We too found a similar effect in HEPES buffer where J^{Cl}_{sm} significantly increased ~ 25% from 11.85 to 14.85 μmol/cm^2/h (Table 3). In addition to HCO_3^-, intracellular CA activity was also required for J^{Ox}_{sm} (Figs. 4A and 5A), a trait shared with the rat distal colon where both $[HCO_3^-]_i$ and CA are crucial mediators for

CO_2-stimulated Cl^- absorption (Charney and Dagher 1996) culminating in the trafficking of AE1 to the apical membrane (Charney et al. 2004a). The underlying signaling mechanism(s) regulating intestinal Cl^- absorption and secretion by the rat colon have not been determined, and while we have yet to identify the transporter(s) responsible for oxalate secretion by the mouse large intestine, it is interesting to consider whether this secretion might share the same regulatory pathway(s) involving $[HCO_3^-]_i$ and CA.

Possible transport mechanisms involved in intestinal oxalate transport

While $[HCO_3^-]_i$ can modulate Cl^- transport, and potentially oxalate secretion, there are additional considerations for interpreting the effects of $[HCO_3^-]_e$ in relation to anion exchange. As HCO_3^- and oxalate are potential substrates on the same transporter, the changes in oxalate fluxes may also be related to direct competition between the two anions (i.e., HCO_3^- (Ox^{2-})/A^- exchange), and/or the dependence of oxalate on HCO_3^- (i.e., HCO_3^-/Ox^{2-} exchange), as illustrated in Figure 8. In the ileum PAT1 is involved in oxalate secretion, specifically J_{sm}^{Ox}, operating as an apical Cl^-/Ox^{2-} exchanger (Freel et al. 2006). Table 2 shows that J_{sm}^{Ox} was undiminished by reducing, or removing, HCO_3^-/CO_2 from the buffer thus indicating PAT1 does not also perform HCO_3^-/Ox^{2-} exchange in the ileum. Even though PAT1 is capable of a variety of transport modes when expressed in *Xenopus* oocytes, including HCO_3^-/Ox^{2-} exchange (Chernova et al. 2005), rates are considered modest relative to Cl^-/Ox^{2-} exchange (Clark et al. 2008), consistent with our observations. Interestingly, recent work has suggested PAT1 contributes to HCO_3^- re-absorption by the jejunum via $HCO_{3\,o}^-/Cl^-_i$ exchange (Xia et al. 2014), and could therefore conceivably perform HCO_3^-/Cl^- (Ox^{2-}) exchange in this part of the small intestine. Unlike the ileum, J_{sm}^{Ox} and consequently net oxalate secretion by the distal colon was clearly dependent on the presence of HCO_3^-/CO_2 (Table 3). One explanation would therefore be if oxalate was dependent on $HCO_{3\,e}^-$ and exiting across the apical membrane via $HCO_{3\,o}^-/Ox^{2-}_i$ exchange (Fig. 8B).

There were also distinct reductions to J_{sm}^{Ox} at 42 mmol/L HCO_3^-, for both the ileum (Table 2) and distal colon (Table 3), which were independent of the change to pH (Tables 4 and 5), and thus considered specific to HCO_3^-. As oxalate secretion at the apical membrane of the distal ileum (via PAT1) is not HCO_3^--dependent, this may represent an impact on a basolateral anion exchanger. For example, oxalate might be competing with HCO_3^- in the serosal bath for entry into the cell by Cl^-/HCO_3^- (Ox^{2-}) exchange, since at 42 mmol/L HCO_3^-, 1.5 μmol/L oxalate would be further out-competed by HCO_3^-. Basolateral membrane vesicles from rabbit ileum identified a distinct SO_4^{2-}/HCO_3^- (Ox^{2-}) exchanger (Knickelbein and Dobbins 1990), but it is not known whether a similar oxalate transporter is present in the mouse ileum. Presently, very little is known about oxalate transport at the basolateral membrane, but a candidate is SAT1 (Sulfate Anion Transporter 1; Slc26a1). SAT1 has been characterized as a

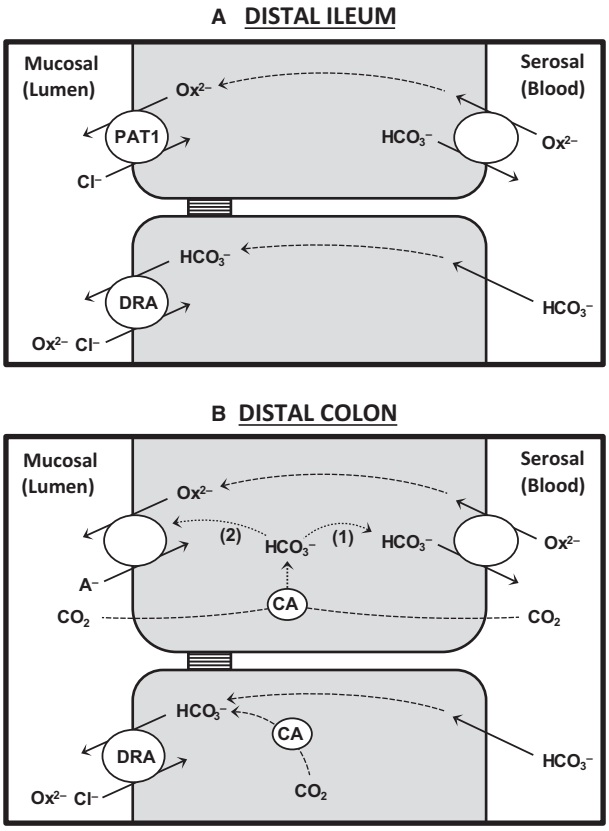

Figure 8. A simple model summarizing some of the known and proposed transcellular pathways for oxalate transport across the distal ileum and distal colon of the mouse intestine. In panel A, oxalate secretion by the ileum was unaffected by the absence of extracellular HCO_3^-/CO_2 and did not require carbonic anhydrase (CA), but does involve Cl^-/Ox^{2-} exchange by PAT1 (Slc26a6), which may be supplied by a basolateral HCO_3^-/Ox^{2-} exchanger. DRA (Slc26a3) contributes to Cl^- (and oxalate) absorption by the ileum driven by the supply of serosal HCO_3^-, and does not depend on CA activity. In panel B, oxalate secretion by the distal colon required intracellular CA activity which may have been supplying HCO_3^- for basolateral HCO_3^-/Ox^{2-} exchange. Elevated CO_2 (via CA and intracellular HCO_3^-) might stimulate oxalate secretion by: (1) promoting basolateral HCO_3^-/Ox^{2-} exchange, and/or (2) influencing the expression of the apical exchanger responsible for oxalate efflux. DRA contributes to the absorption of Cl^- and oxalate by the distal colon, but only Cl^- (not oxalate) absorption demonstrated dependence on intracellular CA activity. See text for further details. A^- = Cl^- or HCO_3^-.

SO_4^{2-}/HCO_3^- (Ox^{2-}) exchanger (Karniski et al. 1998; Krick et al. 2009), expressed in the ileum and proposed to contribute to intestinal SO_4^{2-} absorption and oxalate secretion (Dawson et al. 2010). Although if a transport mode such as this were operating, one could reasonably argue that in HCO_3^-/CO_2 free conditions (with no competition from HCO_3^-), SO_4^{2-}/Ox^{2-} exchange might prevail and thus J_{sm}^{Ox} would have been enhanced, or at the very least sustained, but this was not the case for either the ileum (Table 2) or colon (Table 3). An alternative could be if $HCO_{3\,i}^-$ were the counter-ion for transport across the basolateral membrane (i.e., $HCO_{3\,i}^-/Ox^{2-}{}_o$ exchange), as illustrated in Figure 8 for both the ileum and distal colon. The outwardly directed HCO_3^- gradient driving this exchange would therefore be greatly diminished with extracellular HCO_3^- at 42 mmol/L.

Role of carbonic anhydrase in intestinal oxalate transport

In the intestine, CA can supply intracellular H^+ and HCO_3^- for apical Na^+/H^+ and Cl^-/HCO_3^- exchange, therefore its contribution to NaCl absorption and HCO_3^- secretion is intuitively recognized. We have now extended this role for CA to include oxalate secretion by the mouse distal colon which was dependent on CA activity, evidenced by the ability of ethoxzolamide to abruptly reduce J_{sm}^{Ox} (Figs. 4A and 5A). This was only observed in the presence of extracellular HCO_3^-/CO_2, and not in HEPES buffer (Fig. 6A), ruling out the possibility of a noncatalytic role for CA in oxalate secretion, which has been suggested for apical Cl^-/HCO_3^- exchange in the rat ileum (Charney et al. 2002a), and mouse distal colon (Goldfarb et al. 2000). Of the 16 mammalian CA isozymes identified, the large intestine prominently expresses three, CAI and II (intracellular) and CAIV, an extracellular form bound to the apical membrane (Lonnerholm et al. 1985; Fleming et al. 1995; Goldfarb et al. 2000). With no isoform-specific, or membrane-impermeant, inhibitors commercially available, distinguishing the relative contributions of each is challenging. Utilizing a CAII-KO mouse model and the relatively impermeant CA inhibitor benzolamide, Goldfarb et al. (2000), concluded CAI was required for optimal NaCl absorption by the distal colon. The failure of mucosal N-3500 to abolish net Cl^- absorption, relative to the highly permeant ethoxzolamide (Fig. 5B), would further support this notion of an intracellular CA isoform supporting apical Cl^-/HCO_3^- exchange. The CA-dependence of J_{sm}^{Ox} could be interpreted as a function of the extracellular CAIV facilitating apical HCO_3^-/Ox^{2-} exchange. In this scenario the mucosal application of N-3500 might be expected to reduce J_{sm}^{Ox}, but this was clearly not the case (Fig. 5A), subsequently pointing to a role for an intracellular CA isoform. We suggest that the dependence of oxalate secretion on CA, may be through its supply of $HCO_{3\,i}^-$ to a basolateral HCO_3^-/Ox^{2-} exchanger driving oxalate into the cell, and this may also explain the ability of CO_2 to stimulate oxalate secretion in the distal colon (Fig. 8B).

Another possible mechanism supporting a role for CA in oxalate secretion by the distal colon may be the ability of some CA isoforms, including CAII and CAIV, to physically and functionally interact with a number of the oxalate-transporting exchangers, notably PAT1 (Alvarez et al. 2005) and DRA (Sterling et al. 2002). Figures 4B and 5B show J_{ms}^{Cl} was also simultaneously inhibited by ethoxzolamide and may reflect a reduction in Cl^-/HCO_3^- exchange by DRA. However, despite its role in oxalate absorption (Freel et al. 2013) we noted J_{ms}^{Ox} was not subject to similar inhibition (Figs. 4A and 5A). The characterization of PAT1 as an ileal Cl^-/Ox^{2-} exchanger (Freel et al. 2006), and independent of HCO_3^-/CO_2 (discussed above), would be consistent with the inability of CA to impact J_{sm}^{Ox} in the distal ileum (Fig. 3A), despite the fact that PAT1 can physically bind to CAII (Alvarez et al. 2005). Furthermore, AE1 is another Cl^-/HCO_3^- exchanger capable of physically, as well as functionally, associating with CAII (Sowah and Casey 2011), and involved in CO_2-stimulated Cl^- absorption by the rat distal colon (Charney et al. 2004a), where it is expressed with, and functions alongside, DRA (Rajendran and Binder 2000). In human erythrocytes AE1 can exchange oxalate for Cl^- (Jennings and Adame 1996), but its contribution as either an oxalate or Cl^- transporter in the mouse intestine has not been specifically examined, and there is doubt about whether it is even expressed in the colon (Alper et al. 1999).

Perspectives and summary

Systemic acid-base imbalances lead to coordinated adjustments by various organ systems (cardiovascular, renal, and skeletal) to compensate and restore homeostasis. The contribution of the intestine is easily overlooked, but it too can respond, most notably through the Na^+/H^+ and Cl^-/HCO_3^- exchangers (Charney and Feldman 1984; Charney and Dagher 1996). This is not surprising given the intestine and its resident transporters are involved in handling significant amounts of acidic and basic equivalents each day, and systemic acid-base disturbances are well-documented complications of many gastrointestinal disorders (Charney et al. 1995; Gennari and Weise 2008). There is very little information on the extent to which acute or chronic acid-base disorders will impact intestinal oxalate transport in vivo, and what consequences (if any) this may have for overall oxalate homeostasis. In genetically hypercalciuric rats,

induction of a chronic metabolic acidosis significantly reduced urinary oxalate excretion (Bushinsky et al. 2001). However, similar chronic acid loading of normocalcemic rats did not reveal any significant changes to either urinary oxalate excretion or serum oxalate (Green et al. 2005), suggesting a systemic acidosis does not alter renal oxalate handling or oxalate metabolism. The DRA-KO mouse is a model of the disease congenital chloride diarrhea (CCD) and exhibits a chronic metabolic alkalosis with respiratory compensation (Walker et al. 2008; Xiao et al. 2014). In our report on this model (Freel et al. 2013), urinary oxalate excretion and serum oxalate were decreased, associated with an induction of net oxalate secretion by the intestine. We emphasize that this change in transport was due to a reduction in J_{ms}^{Ox} from the absence of DRA, rather than enhanced secretion, but we did record a (nonsignificant) 40% increase in J_{sm}^{Ox} by the distal colon ($P = 0.10$). The intestinal phenotype and urine pH of these mice suggested they harbored the same acid-base disturbance but we did not perform a blood-gas analysis to verify their overall acid-base status. The impact of CCD on the mass-balance of oxalate in humans has not been assessed. A survey of 35 patients diagnosed with, and treated for, this disease found urinary oxalate excretion was within the "normal" range (Wedenoja et al. 2008), however, only very few of these individuals exhibited any systemic acid-base abnormalities (median serum HCO_3^- = 25 mmol/L, blood pH and P_{CO_2} were not reported). Finally, CA inhibitors, such as acetazolamide, are used clinically for treating various disorders including glaucoma, edema, seizures, and altitude sickness. A potential complication for patients is the development of metabolic acidosis and a propensity for calcium phosphate kidney stone formation, associated with increased urine pH and hypocitraturia (Matlaga et al. 2003; Mirza et al. 2009). The impacts of CA inhibitors on oxalate homeostasis in vivo, however, are limited and inconclusive. A significant rise in urinary oxalate excretion and some mixed calcium phosphate/oxalate stones have been reported in patients taking acetazolamide (Ahlstrand and Tiselius 1987), whereas other studies with CA-inhibiting drugs have revealed no changes to urinary oxalate handling (Higashihara et al. 1991; Welch et al. 2006; Kaplon et al. 2011).

In summary, oxalate secretion (but not Cl^- absorption) by the mouse distal colon was acutely stimulated by increasing P_{CO_2} in vitro. The secretory pathway, J_{sm}^{Ox}, was found to be exclusively responsive to changes in HCO_3^-, CO_2, and dependent on CA activity, but not pH. These results strongly suggest oxalate secretion by this segment is specifically regulated by CO_2. In contrast, net oxalate secretion by the ileum was generally unresponsive to alterations in these same acid-base variables. These findings highlight some of the distinct segmental heterogeneity in oxalate transport that exists along the intestine, but also provides important new insights into the characteristics of the underlying transport mechanisms and how they might be regulated, thus helping to direct future work in this area.

Acknowledgments

The authors wish to thank Kristina Fernandez, Tara Braun, Tisha Van Pelt and Heran Getachew for technical assistance and animal husbandry. We are also very grateful to Dr. Robert W. Freel and Dr. David N. Silverman for valuable discussions and helpful advice during the course of this work.

Conflict of Interest

None declared.

References

Ahlstrand, C., and H. G. Tiselius. 1987. Urine composition and stone formation during treatment with acetazolamide. Scand. J. Urol. Nephrol. 21:225–228.

Alper, S. L., H. Rossmann, S. Wilhelm, A. K. Stuart-Tilley, B. E. Shmukler, and U. Seidler. 1999. Expression of AE2 anion exchanger in mouse intestine. Am. J. Physiol. Gastrointest. Liver Physiol. 277:G321–G332.

Alvarez, B. V., G. L. Vilas, and J. R. Casey. 2005. Metabolon disruption: a mechanism that regulates bicarbonate transport. EMBO J. 24:2499–2511.

Armbrecht, H. J., M. A. Boltz, and T. L. Hodam. 2002. Differences in intestinal calcium and phosphate transport between low and high bone density mice. Am. J. Physiol. Gastrointest. Liver Physiol. 282:G130–G136.

Bushinsky, D. A., M. D. Grynpas, and J. R. Asplin. 2001. Effect of acidosis on urine supersaturation and stone formation in genetic hypercalciuric stone-forming rats. Kidney Int. 59:1415–1423.

Charney, A. N., and P. C. Dagher. 1996. Acid-base effects on colonic electrolyte transport revisited. Gastroenterology 111:1358–1368.

Charney, A. N., and G. M. Feldman. 1984. Systemic acid-base-disorders and intestinal electrolyte transport. Am. J. Physiol. Gastrointest. Liver Physiol. 247:G1–G12.

Charney, A. N., J. D. Wagner, G. J. Birnbaum, and J. N. Johnstone. 1986. Functional role of carbonic-anhydrase in intestinal electrolyte transport. Am. J. Physiol. Gastrointest. Liver Physiol. 251:G682–G687.

Charney, A. N., D. S. Goldfarb, and R. W. Egnor. 1991. Effects of pH and cyclic adenosine-monophosphate on ileal electrolyte transport in the rat and rabbit. Gastroenterology 100:410–418.

Charney, A. N., D. S. Goldfarb, and P. C. Dagher. 1995. Metabolic disorders associated with gastrointestinal disease. Pp. 813–836 *in* A. I. Arieff and R. A. DeFronzo, eds. Fluid, electrolyte, and acid-base disorders. Churchill Livingstone, New York.

Charney, A. N., J. Alexander-Chacko, R. Gummaconda, and R. W. Egnor. 2002a. Non-catalytic role of carbonic anhydrase in rat intestinal absorption. Biochim. Et Biophys. Acta-General Subjects 1573:141–148.

Charney, A. N., R. W. Egnor, J. Alexander-Chacko, N. Cassai, and G. S. Sidhu. 2002b. Acid-base effects on intestinal Na^+ absorption and vesicular trafficking. Am. J. Physiol.-Cell Physiol. 283:C971–C979.

Charney, A. N., R. W. Egnor, D. Henner, H. Rashid, N. Cassai, and G. S. Sidhu. 2004a. Acid-base effects on intestinal Cl^- absorption and vesicular trafficking. Am. J. Physiol.-Cell Physiol. 286:C1062–C1070.

Charney, A. N., R. W. Egnor, K. A. Steinbrecher, and M. B. Cohen. 2004b. Effect of secretagogues and pH on intestinal transport in guanylin-deficient mice. Biochim. Et Biophys. Acta-General Subjects 1671:79–86.

Chernova, M. N., L. W. Jiang, D. J. Friedman, R. B. Darman, H. Lohi, J. Kere, et al. 2005. Functional comparison of mouse slc26a6 anion exchanger with human SLC26A6 polypeptide variants – Differences in anion selectivity, regulation, and electrogenicity. J. Biol. Chem. 280:8564–8580.

Clark, J. S., D. H. Vandorpe, M. N. Chernova, J. F. Heneghan, A. K. Stewart, and S. L. Alper. 2008. Species differences in Cl^- affinity and in electrogenicity of SLC26A6-mediated oxalate/Cl^- exchange correlate with the distinct human and mouse susceptibilities to nephrolithiasis. J. Physiol.-London 586:1291–1306.

Dagher, P. C., L. Balsam, J. T. Weber, R. W. Egnor, and A. N. Charney. 1992. Modulation of chloride secretion in the rat colon by intracellular bicarbonate. Gastroenterology 103:120–127.

Dagher, P. C., T. Z. Morton, C. S. Joo, A. Tagliettakohlbrecher, R. W. Egnor, and A. N. Charney. 1994. Modulation of secretagogue-induced chloride secretion by intracellular bicarbonate. Am. J. Physiol. Gastrointest. Liver Physiol. 266:G929–G934.

Dawson, P. A., C. S. Russell, S. Lee, S. C. McLeay, J. M. van Dongen, D. M. Cowley, et al. 2010. Urolithiasis and hepatotoxicity are linked to the anion transporter Sat1 in mice. J. Clin. Invest. 120:706–712.

Delacruz, J., R. Mikulski, C. Tu, Y. Li, H. Wang, K. T. Shiverick, et al. 2010. Detecting extracellular carbonic anhydrase activity using membrane inlet mass spectrometry. Anal. Biochem. 403:74–78.

Fleming, R. E., S. Parkkila, A. K. Parkkila, H. Rajaniemi, A. Waheed, and W. S. Sly. 1995. Carbonic anhydrase IV expression in rat and human gastrointestinal tract regional, cellular, and subcellular localization. J. Clin. Invest. 96:2907–2913.

Flores, C. A., L. P. Cid, and F. V. Sepulveda. 2010. Strain-dependent differences in electrogenic secretion of electrolytes across mouse colon epithelium. Exp. Physiol. 95:686–698.

Freel, R. W., M. Hatch, M. Green, and M. Soleimani. 2006. Ileal oxalate absorption and urinary oxalate excretion are enhanced in Slc26a6 null mice. Am. J. Physiol. Gastrointest. Liver Physiol. 290:G719–G728.

Freel, R. W., J. M. Whittamore, and M. Hatch. 2013. Transcellular oxalate and Cl^- absorption in mouse intestine is mediated by the DRA anion exchanger Slc26a3, and DRA deletion decreases urinary oxalate. Am. J. Physiol. Gastrointest. Liver Physiol. 305:G520–G527.

Gawenis, L. R., E. M. Bradford, S. L. Alper, V. Prasad, and G. E. Shull. 2010. AE2 Cl^-/HCO_3^- exchanger is required for normal cAMP-stimulated anion secretion in murine proximal colon. Am. J. Physiol. Gastrointest. Liver Physiol. 298:G493–G503.

Gennari, F. J., and W. J. Weise. 2008. Acid-Base Disturbances in Gastrointestinal Disease. Clin. J. Am. Soc. Nephrol. 3:1861–1868.

Goldfarb, D. S., R. W. Egnor, and A. N. Charney. 1988. Effects of acid-base variables on ion-transport in rat colon. J. Clin. Invest. 81:1903–1910.

Goldfarb, D. S., W. S. Sly, A. Waheed, and A. N. Charney. 2000. Acid-base effects on electrolyte transport in CA II-deficient mouse colon. Am. J. Physiol. Gastrointest. Liver Physiol. 278:G409–G415.

Green, M. L., M. Hatch, and R. W. Freel. 2005. Ethylene glycol induces hyperoxaluria without metabolic acidosis in rats. Am. J. Physiol. Renal Physiol. 289:F536–F543.

Hatch, M., and R. W. Freel. 2005. Intestinal transport of an obdurate anion: oxalate. Urol. Res. 33:1–16.

Hatch, M., and R. W. Freel. 2008. The roles and mechanisms of intestinal oxalate transport in oxalate homeostasis. Semin. Nephrol. 28:143–151.

Hatch, M., R. W. Freel, and N. D. Vaziri. 1994. Mechanisms of oxalate absorption and secretion across the rabbit distal colon. Pflugers Archiv: Euro. J. Physiol. 426:101–109.

Hatch, M., A. Gjymishka, E. C. Salido, M. J. Allison, and R. W. Freel. 2011. Enteric oxalate elimination is induced and oxalate is normalized in a mouse model of primary hyperoxaluria following intestinal colonization with *Oxalobacter*. Am. J. Physiol. Gastrointest. Liver Physiol. 300: G461–G469.

Higashihara, E., K. Nutahara, T. Takeuchi, N. Shoji, M. Araie, and Y. Aso. 1991. Calcium-metabolism in acidotic patients induced by carbonic-anhydrase inhibitors – responses to citrate. J. Urol. 145:942–948.

Hoglund, P., S. Haila, J. Socha, L. Tomaszewski, U. SaarialhoKere, M. L. KarjalainenLindsberg, K. Airola, C. Holmberg, A. delaChapelle, and J. Kere. 1996. Mutations of the down-regulated in adenoma (DRA) gene cause congenital chloride diarrhoea. Nat. Genet. 14: 316–319.

Jennings, M. L., and M. F. Adame. 1996. Characterization of oxalate transport by the human erythrocyte band 3 protein. J. Gen. Physiol. 107:145–159.

Jiang, Z. R., J. R. Asplin, A. P. Evan, V. M. Rajendran, H. Velazquez, T. P. Nottoli, et al. 2006. Calcium oxalate urolithiasis in mice lacking anion transporter Slc26a6. Nat. Genet. 38:474–478.

Kaplon, D. M., K. L. Penniston, and S. Y. Nakada. 2011. Patients with and without prior urolithiasis have hypocitraturia and incident kidney stones while on topiramate. Urol. 77:295–298.

Karniski, L. P., M. Lotscher, M. Fucentese, H. Hilfiker, J. Biber, and H. Murer. 1998. Immunolocalization of sat-1 sulfate/oxalate/bicarbonate anion exchanger in the rat kidney. Am. J. Physiol.-Renal Physiol. 275:F79–F87.

Kato, A., and M. F. Romero. 2011. Regulation of electroneutral NaCl absorption by the small intestine. Annu. Rev. Physiol. 73:261–281.

Knickelbein, R. G., and J. W. Dobbins. 1990. Sulfate and oxalate exchange for bicarbonate across the basolateral membrane of rabbit ileum. Am. J. Physiol. Gastrointest. Liver Physiol. 259:G807–G813.

Krick, W., N. Schnedler, G. Burckhardt, and B. C. Burckhardt. 2009. Ability of sat-1 to transport sulfate, bicarbonate, or oxalate under physiological conditions. Am. J. Physiol. Renal Physiol. 297:F145–F154.

Kurtin, P., and A. N. Charney. 1984. Intestinal ion-transport and intracellular pH during acute respiratory alkalosis and acidosis. Am. J. Physiol. Gastrointest. Liver Physiol. 247: G24–G31.

Lonnerholm, G., O. Selking, and P. J. Wistrand. 1985. Amount and distribution of carbonic-anhydrases CA-I and CA-II in the gastrointestinal-tract. Gastroenterology 88:1151–1161.

Matlaga, B. R., O. D. Shah, and D. G. Assimos. 2003. Drug-induced urinary calculi. Rev. Urol. 5:227–231.

Mirza, N., A. G. Marson, and M. Pirmohamed. 2009. Effect of topiramate on acid-base balance: extent, mechanism and effects. Br. J. Clin. Pharmacol. 68:655–661.

Rajendran, V. M., and H. J. Binder. 1999. Distribution and regulation of apical Cl/anion exchanges in surface and crypt cells of rat distal colon. Am. J. Physiol. Gastrointest. Liver Physiol. 276:G132–G137.

Rajendran, V. M., and H. J. Binder. 2000. Characterization and molecular localization of anion transporters in colonic epithelial cells. Pp. 15–29 *in* J. D. Schulzke, M. Fromm, E. O. Riecken and H. J. Binder, eds. Epithelial transport and barrier function: pathomechanisms in gastrointestinal disorders. New York Academy of Sciences, New York, NY.

Rajendran, V. M., J. Black, T. A. Ardito, P. Sangan, S. L. Alper, C. Schweinfest, et al. 2000. Regulation of DRA and AE1 in rat colon by dietary Na depletion. Am. J. Physiol. Gastrointest. Liver Physiol. 279:G931–G942.

Robijn, S., B. Hoppe, B. A. Vervaet, P. C. D'Haese, and A. Verhulst. 2011. Hyperoxaluria: a gut-kidney axis? Kidney Int. 80:1146–1158.

Schweinfest, C. W., D. D. Spyropoulos, K. W. Henderson, J. H. Kim, J. M. Chapman, S. Barone, et al. 2006. slc26a3 (dra)-deficient mice display chloride-losing diarrhea, enhanced colonic proliferation, and distinct up-regulation of ion transporters in the colon. J. Biol. Chem. 281:37962–37971.

Siggaard-Andersen, O. 1974. The acid-base status of the blood. William & Wilkins Co., Baltimore, p. 229.

Simpson, J. E., C. W. Schweinfest, G. E. Shull, L. R. Gawenis, N. M. Walker, K. T. Boyle, et al. 2007. PAT-1 (Slc26a6) is the predominant apical membrane Cl^-/HCO_3^- exchanger in the upper villous epithelium of the murine duodenum. Am. J. Physiol. Gastrointest. Liver Physiol. 292:G1079–G1088.

Simpson, J. E., N. M. Walker, C. T. Supuran, M. Soleimani, and L. L. Clarke. 2010. Putative anion transporter-1 (Pat-1, Slc26a6) contributes to intracellular pH regulation during H^+-dipeptide transport in duodenal villous epithelium. Am. J. Physiol. Gastrointest. Liver Physiol. 298:G683–G691.

Singh, A. K., M. Sjoblom, W. Zheng, A. Krabbenhoft, B. Riederer, B. Rausch, et al. 2008. CFTR and its key role in *in vivo* resting and luminal acid-induced duodenal HCO_3^- secretion. Acta Physiol. 193:357–365.

Singh, A. K., B. Riederer, M. M. Chen, F. Xiao, A. Krabbenhoft, R. Engelhardt, et al. 2010. The switch of intestinal Slc26 exchangers from anion absorptive to HCO_3^- secretory mode is dependent on CFTR anion channel function. Am. J. Physiol.-Cell Physiol. 298:C1057–C1065.

Sowah, D., and J. R. Casey. 2011. An intramolecular transport metabolon: fusion of carbonic anhydrase II to the COOH terminus of the Cl^-/HCO_3^- exchanger, AE1. Am. J. Physiol. Cell Physiol. 301:C336–C346.

Sterling, D., N. J. D. Brown, C. T. Supuran, and J. R. Casey. 2002. The functional and physical relationship between the DRA bicarbonate transporter and carbonic anhydrase II. Am. J. Physiol. Cell Physiol. 283:C1522–C1529.

Talbot, C., and C. Lytle. 2010. Segregation of Na/H exchanger-3 and Cl/HCO_3 exchanger SLC26A3 (DRA) in rodent cecum and colon. Am. J. Physiol. Gastrointest. Liver Physiol. 299:G358–G367.

Townsend, P. D., P. M. Holliday, S. Fenyk, K. C. Hess, M. A. Gray, D. R. W. Hodgson, et al. 2009. Stimulation of Mammalian G-protein-responsive Adenylyl Cyclases by Carbon Dioxide. J. Biol. Chem. 284:784–791.

Uchiyama, H., H. Hayashi, K. Tanji, O. Sugimoto, and Y. Suzuki. 2007. pH stat studies on bicarbonate secretion in the isolated mouse ileum. Biomed. Res. Tokyo 28:239–246.

Vaccarezza, S. G., and A. N. Charney. 1988. Acid-base effects on ileal sodium-chloride absorption *in vitro*. Am. J. Physiol. Gastrointest. Liver Physiol. 254:G329–G333.

Wagner, J. D., P. Kurtin, and A. N. Charney. 1986. Effect of systemic acid-base-disorders on ileal intracellular pH and ion-

transport. Am. J. Physiol. Gastrointest. Liver Physiol. 250: G588–G593.

Walker, N. M., J. E. Simpson, P. F. Yen, R. K. Gill, E. V. Rigsby, J. M. Brazill, et al. 2008. Down-regulated in adenoma Cl/HCO_3 exchanger couples with Na/H exchanger 3 for NaCl absorption in murine small intestine. Gastroenterology 135:1645–1653.

Walker, N. M., J. E. Simpson, E. E. Hoover, J. M. Brazill, C. W. Schweinfest, M. Soleimani, et al. 2011. Functional activity of Pat-1 (Slc26a6) Cl^-/HCO_3^- exchange in the lower villus epithelium of murine duodenum. Acta Physiol. 201: 21–31.

Wang, Z. H., S. Petrovic, E. Mann, and M. Soleimani. 2002. Identification of an apical Cl^-/HCO_3^- exchanger in the small intestine. Am. J. Physiol. Gastrointest. Liver Physiol. 282: G573–G579.

Wang, Z. H., T. Wang, S. Petrovic, B. G. Tuo, B. Riederer, S. Barone, et al. 2005. Renal and intestinal transport defects in Slc26a6-null mice. Am. J. Physiol. Cell Physiol. 288: C957–C965.

Wedenoja, S., T. Ormala, U. B. Berg, S. F. E. Halling, H. Jalanko, R. Karikoski, et al. 2008. The impact of sodium chloride and volume depletion in the chronic kidney disease of congenital chloride diarrhea. Kidney Int. 74:1085–1093.

Welch, B. J., D. Graybeal, O. W. Moe, N. M. Maalouf, and K. Sakhaee. 2006. Biochemical and stone-risk profiles with topiramate treatment. Am. J. Kidney Dis. 48:555–563.

Whittamore, J. M., R. W. Freel, and M. Hatch. 2013. Sulfate secretion and chloride absorption are mediated by the anion exchanger DRA (Slc26a3) in the mouse cecum. Am. J. Physiol. Gastrointest. Liver Physiol. 305:G172–G184.

Xia, W. L., Q. Yu, B. Riederer, A. K. Singh, R. Engelhardt, S. Yeruva, et al. 2014. The distinct roles of anion transporters Slc26a3 (DRA) and Slc26a6 (PAT-1) in fluid and electrolyte absorption in the murine small intestine. Pflugers Archiv: Euro. J. Physiol. 466:1541–1556.

Xiao, F., Q. Yu, J. Li, M. E. V. Johansson, A. K. Singh, W. Xia, et al. 2014. Slc26a3 deficiency is associated with loss of colonic HCO_3^- secretion, absence of a firm mucus layer and barrier impairment in mice. Acta Physiol. 211:161–175.

Zhang, H., N. Ameen, J. E. Melvin, and S. Vidyasagar. 2007. Acute inflammation alters bicarbonate transport in mouse ileum. J. Physiol. 581:1221–1233.